High-frequency Hall Effect and Transverse Electric Galvanomagnetic Waves in Current-biased 2D Electron Systems[1]

A. S. Petrov[2], D. Svintsov

Laboratory of 2D Materials for Optoelectronics, Moscow Institute of Physics and Technology, 141701 Dolgoprudny, Russia

We derive the *electrodynamic* conductivity tensor for 2DESs with dc drift with account for the high-frequency Hall effect (interaction of dc current with ac magnetic field). We demonstrate the limitations of the *quasistatic* approach which neglects this effect. With the help of *electrodynamic* conductivity we find a novel two-dimensional transverse electric (TE) electromagnetic mode. This mode is non-reciprocal with dispersion $\omega = \mathbf{k}\mathbf{u}_0$ and manifests itself in lowering the reflection coefficient of 2DES at the resonance frequency. In addition, we predict birefringence of an incident evanescent TE wave on a 2DES system with drift and find hints of Cerenkov amplification in the low frequency limit. We discuss the limitng cases when the quasistatic approach is suitable.

Introduction. Electromagnetic (EM) waves in isotropic dielectrics are transverse. If we introduce conducting media (plasma) into a dielectric environment, EM waves become more complex and can be described as a superposition of TM (transverse magnetic) and TE (transverse electric) modes. The former are commonly known as plasma waves, or plasmons, as they incorporate not only oscillations of EM fields, but also oscillations of electric charge density and current in the conducting media. In turn, TE waves usually involve only current, and not charge density, oscillations[3].

In bulk isotropic plasmas neither TM, nor TE modes can propagate at frequencies ω below the plasma frequency ω_{3d} even in the absence of dissipation. At the same time, in anisotropic media this condition is greatly relaxed. For example, bulk plasmas in a magnetic field support helicons [1, 2], low frequency TE modes with high Q-factor ($\omega\tau \ll 1$, where τ is effective charge carrier momentum relaxation time). Helicons were first observed in sodium [3] and a year later were assosiated with atmospheric whistlers [4], $\sim 10\,\mathrm{kHz}$ oscillations that travel along the Earth's magnetic field and can circumnavigate the Earth several times before fading.

While application of an external magnetic field is the most straightforward way to introduce TE modes to a plasma, it may not be the most efficient one. The less common options include passage of a constant electric current through the sample, which leads to formation of ultra-low frequency galvanomagnetic waves (GMWs). These waves were predicted by Morozov and Shubin in 1964 [5] and observed by Kopylov in 1979 [6] in Bi monocrystals. The term *magnetic* in GMW reflects the magnetic nature of the restoring force in this wave. The spectrum of GMWs is given by a simple relation [6]

$$\omega = \mathbf{k}\mathbf{u}_0 - ic^2 k^2/4\pi\sigma_v, \tag{1}$$

where $\mathbf{k}$ is the wave vector, $\mathbf{u}_0$ is the dc carrier drift velocity, c is the speed of light, σ_v is the static Drude volume conductivity. Plugging the typical Bi parameters into Eq. (1) gives $\nu = \mathrm{Re}\,\omega \simeq 600\,\mathrm{rad/s}$; $\mathrm{Im}\,\omega \simeq \simeq -100\,\mathrm{rad/s}$ while the effective momentum relaxation rate $1/\tau$ is the order of THz. In addition to this rather unusual behavior, GMWs are intrinsically non-reciprocal: Eq. (1) dictates that the wavevector must be co-directional with the drift velocity, which was verified in the experiment [6]. Notably, similar properties are shared by thermomagnetic waves (TMWs) that propagate along a temperature gradient in bulk semiconductors [7, 8], but these modes lie out of the scope of our paper.

The two given examples (helicons and GMWs) convince us that long travelpaths at low $\omega\tau$-factors represent a natural footprint of TE modes. This happens due to the fact that the current and electric field of TE waves

---

[3]This statement can be easily checked from the continuity equation $i\omega\rho = (i\mathbf{k}, \hat{\sigma}\mathbf{E})$. Usually the conductivity tensor is diagonal and for TE modes we immediately obtain $\rho = 0$.

are phase-shifted by $\pi/2$, the shift being independent of $\mathrm{Re}\,\sigma$[4]. Thus, TE electromagnetic waves in bulk plasmas are remarkable objects with promising applications due to long travelpaths.

Despite having bright properties in bulk plasmas, TE modes are practically unexplored in two-dimensional electron systems (2DESs). The reason for this might be the fact that common 2DESs (with parabolic electron dispersion) cannot support TE modes. Indeed, Fal'ko and Khmel'nitskii showed [9] that a TE mode can propagate along a 2DES only if the 2DES's surface conductivity σ has capacitive nature, i.e.,

$$\mathrm{Im}\,\sigma(\omega) < 0, \qquad (2)$$

temporal dependence $e^{-i\omega t}$ is assumed throughout the paper. Only recently, in 2007, S. A. Mikhailov and K. Ziegler noticed [10] that unique electron-hole plasma in graphene can be used to fulfill this seemingly improbable condition and thus open the prospect for TE mode observation. This mode was experimentaly probed in graphene nanostructure several years later [11]. Further works studied graphene TE plasmons in the presence of dc drift pependicular to the wave vector [12, 13].

Still, TE modes in anisotropic 2DESs with parabolic spectrum are scarcely investigated. Thus, we are aware only of some signatures for existence of transverse magnetosound waves in viscous 2D electronic fluids [14–16].

In this paper we demonstrate that the interaction of dc charge carrier drift in a 2DES with TE wave's magnetic field (which can be called the high-frequency Hall effect) has a pronounced impact on the 2DES's ac conductivity and electromagnetic properties. We derive the corresponding *electrodynamic* conductivity tensor and predict the formation of 2D galvanomagnetic waves analogous to (1). We establish field distribution of these modes and examine the response of 2DESs to exciting radiation with account for this interaction. In addition, we show that this effect is responsible for birefringence of an evanescent TE wave incident on a 2DES and find hints of Cerenkov amplification in the low frequency limit.

1. Theoretical model. We consider an infinite two-dimensional electron system (2DES) with homogeneous carrier density n_0 that is sandwiched between two materials with permittivities ε_i and permeabilities $\mu_i, i = 1, 2$. A constant dc current $j_0 = n_0 u_0$ flows across the 2DES (Fig. 1).

1.1. 2DES electromagnetic conductivity in the presence of drift. A general property of any system that en-

---

[4] This fact can be proved by combining the Maxwell's induction law and Ampere's law to give $q^2\mathbf{E} = 4\pi i\omega/c^2\mathbf{j}$ for TE waves.
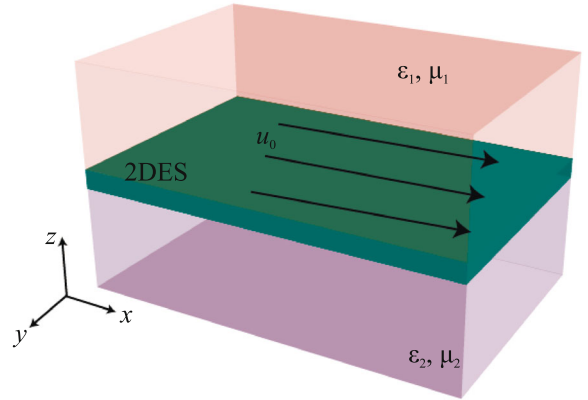

Fig. 1. (Color online) Schematic view of a host system for two-dimensional GMW. A 2DES with homogeneous carrier density is subject to electrical potential gradient in x-direction, which leads to formation of dc current with carrier drift velocity u_0. The structure is sandwiched between dielectrics with permittivities $\varepsilon_1, \varepsilon_2$ and permeabilities μ_1, μ_2. The main part of the paper deals with the case $\varepsilon_1 = \varepsilon_2$, $\mu_1 = \mu_2 = 1$ for simplicity

codes its response to external electromagnetic fields and thus carries information about the system's eigenmodes is the dielectric function or, equivalently, conductivity. We derive the conductivity of the system under consideration from the linearized Euler's equation

$$-i\tilde{\omega}m\mathbf{v}_\omega = \mathbf{F}_L + m(\mathbf{u}_0, \nabla)\mathbf{v}_\omega, \qquad (3)$$

where $\mathbf{F}_L$ is the Lorentz force, m is the electron effective mass, $\tilde{\omega} = \omega + i/\tau_p$, $1/\tau_p$ is the effective carrier momentum relaxation rate with respect to collisions with phonons or impurities, and $\mathbf{v}_\omega$ is the temporal Fourier component of the carrier velocity in plasma wave. Usually in the absence of external magnetic field only the electric component of the Lorentz force acts on charge carriers. However, when the background drift is present, the magnetic component is also essential; in particular, this component leads to the formation of electromagnetic (non-potential) plasma instabilities in gaseous plasmas [17] or semiconductors [18]. Keeping this in mind, we rewrite Eq. (3) as follows:

$$-i\tilde{\omega}m\mathbf{v}_\omega = -e\mathbf{E}_\omega - \frac{e}{c}\mathbf{u}_0 \times \mathbf{B}_\omega + m(\mathbf{u}_0, \nabla)\mathbf{v}_\omega, \quad (4)$$

where $\mathbf{E}_\omega$ and $\mathbf{B}_\omega$ are the temporal Fourier components of electric and magnetic fields of the plasma wave, respectively.

At this moment we perform the following operations: (1) apply the Faraday's law of induction and express $\mathbf{B}_\omega$ via $\mathbf{E}_\omega$, (2) perform the 2d spatial Fourier transform in the 2DES plane and (3) express the plasma wave current $\mathbf{j} = n_0\mathbf{v} + \mathbf{u}_0 n$ ($\mathbf{v}$ and n are the plasma wave velocity and carrier density) via the electric field:

$$\mathbf{j} = \hat{\sigma}^{ED}\mathbf{E}, \qquad (5)$$

where all the plasma wave-associated quatities are assumed to be their $(\mathbf{k}, \omega)$-Fourier compoments, $\mathbf{k}$ is the in-plane wave vector, and the electrodynamic conductivity tensor $\hat{\sigma}^{ED}$ is given by:

$$\hat{\sigma}^{ED} = \frac{\sigma_0}{\tilde{\omega} - k_x u_0} \begin{pmatrix} \dfrac{\omega^2 + (k_y u_0)^2}{(\omega - k_x u_0)} & k_y u_0 \\ k_y u_0 & \omega - k_x u_0 \end{pmatrix}, \quad (6)$$

where $\sigma_0 = ie^2 n_0 / m\omega$ is the free 2DES dynamic conductivity. It is instructive to compare $\hat{\sigma}^{ED}$ with the quasistatic conductivity tensor $\hat{\sigma}^{QS}$ (when the interaction between the ac magnetic field and dc drift is neglected):

$$\hat{\sigma}^{QS} = \frac{\sigma_0}{\tilde{\omega} - k_x u_0} \begin{pmatrix} \dfrac{\omega^2}{(\omega - k_x u_0)} & \dfrac{\omega k_y u_0}{(\omega - k_x u_0)} \\ 0 & \omega \end{pmatrix}. \quad (7)$$

The above tensor is non-symmetrical, which implies chirality of such a system (see Supplementary materials). Surely, steady current cannot introduce chirality, so the quasistatic approximation (7) should be used carefully. Still, this approximation works well as long as

$$\mathbf{j}_\omega^{ED} - \mathbf{j}_\omega^{QS} \propto \frac{u_0}{c}\mathbf{B}_\omega \to 0. \qquad (8)$$

Thus, all the previous results obtained for TM plasmons ($\mathbf{k}\|\mathbf{E}_\omega$, $\mathbf{B}_\omega = 0$) in 2DESs with drift (e.g., [19–24]) remain valid, as well as some rigorous electrodynamic models constructed for special cases, e.g. $E_y = 0$ in [25].

1.2. The search for eigen modes. Now our goal is to search for eigen modes in the scheme of Fig. 1 with 2DES conductivity $\hat{\sigma}^{ED}$. For this reason we assume that the 2DES is located at $z = 0$, define area $z > 0$ be area I and area $z < 0$ be area II, and then search for eigenmodes in the form of linear combination of TE and TM waves:

$$\mathbf{E}_{\mathrm{I}} = \left[\mathrm{TE}_{\mathrm{I}} \begin{pmatrix} -\sin\alpha \\ \cos\alpha \\ 0 \end{pmatrix} + \mathrm{TM}_{\mathrm{I}} \begin{pmatrix} -ik_z\cos\alpha/k \\ -ik_z\sin\alpha/k \\ 1 \end{pmatrix} \right] \mathcal{E}_{\mathrm{I}}(\mathbf{r}, t);$$
$$(9)$$

$$\mathbf{E}_{\mathrm{II}} = \left[\mathrm{TE}_{\mathrm{I}} \begin{pmatrix} -\sin\alpha \\ \cos\alpha \\ 0 \end{pmatrix} + \mathrm{TM}_{\mathrm{II}} \begin{pmatrix} ik_z\cos\alpha/k \\ ik_z\sin\alpha/k \\ 1 \end{pmatrix} \right] \mathcal{E}_{\mathrm{II}}(\mathbf{r}, t),$$
$$(10)$$

where $\mathrm{TE}_{\mathrm{I,II}}$ and $\mathrm{TM}_{\mathrm{I,II}}$ are the amplitudes of TE and TM electric field in the corresponding areas,

$$\mathcal{E}_{\mathrm{I,II}}(\mathbf{r}, t) = \exp\left(ik\cos\alpha x + ik\sin\alpha y \mp k_z z - i\omega t\right), \qquad (11)$$

α is the angle between the wave vector and the drift direction, $k_z = \sqrt{k^2 - k_0^2}$, and $k_0 = \sqrt{\varepsilon}\omega/c$.

Then we evaluate the corresponding magnetic fields via the Faraday's law and apply the boundary conditions on the tangential components of the electric and magnetic fields. As a result, we arrive at a linear system which acquires diagonal form if we change variables to $\mathrm{TE}_\pm = 1/2(\mathrm{TE}_{\mathrm{I}} \pm \mathrm{TE}_{\mathrm{II}})$ and $\mathrm{TM}_\pm = 1/2(\mathrm{TM}_{\mathrm{I}} \pm \mathrm{TM}_{\mathrm{II}})$:

$$\begin{pmatrix} \hat{M}_1 & 0 \\ 0 & \hat{M}_2 \end{pmatrix} \begin{pmatrix} \{\mathrm{TE}_-, \mathrm{TM}_+\}^T \\ \{\mathrm{TE}_+, \mathrm{TM}_-\}^T \end{pmatrix} = 0, \qquad (12)$$

where the upper index T denotes transposition operation,

$$\hat{M}_1 = \begin{pmatrix} -\sin\alpha & -i\kappa_z\cos\alpha/\kappa \\ \cos\alpha & -i\kappa_z\sin\alpha/\kappa \end{pmatrix}, \qquad (13)$$

$\kappa_z = k_z/k_0$, $\kappa = k/k_0$,

$$\hat{M}_2 = \begin{pmatrix} -i\sin\alpha\Sigma_{xx} + i\cos\alpha\Sigma_{xy} + \kappa_z\sin\alpha & \cos\alpha\Sigma_{xx}\kappa_z/\kappa + \sin\alpha\Sigma_{xy}\kappa_z/\kappa - i\cos\alpha/\kappa \\ -i\sin\alpha\Sigma_{yx} + i\cos\alpha\Sigma_{yy} - \kappa_z\cos\alpha & \cos\alpha\Sigma_{yx}\kappa_z/\kappa + \sin\alpha\Sigma_{yy}\kappa_z/\kappa - i\sin\alpha/\kappa \end{pmatrix}, \qquad (14)$$

and $\Sigma_{ij} = 2\pi\sigma_{ij}/c$.

It can be easily checked that $\det\hat{M}_1 = 0$ only when $k_z = 0$, which makes the waves divergent at $z = \pm\infty$. So, we conclude that $\mathrm{TE}_- = \mathrm{TM}_+ = 0$, or $\mathrm{TE}_{\mathrm{I}} = \mathrm{TE}_{\mathrm{II}} = \mathrm{TE}$, $\mathrm{TM}_{\mathrm{I}} = -\mathrm{TM}_{\mathrm{II}} = \mathrm{TM}$, and arrive at

$$\hat{M}_2 \begin{pmatrix} \mathrm{TE} \\ \mathrm{TM} \end{pmatrix} = 0. \qquad (15)$$

Thus, the dispersion equation reads

$$\det\hat{M}_2 = 0. \qquad (16)$$

First, let us take the simple limit $\alpha = 0$ (the wave vector is parallel to drift). Then $\Sigma_{xy} = \Sigma_{yx} = 0$ and Eq. (16) simplifies to

$$\begin{pmatrix} 0 & \Sigma_{xx}\kappa_z - i \\ i\Sigma_{yy} - \kappa_z & 0 \end{pmatrix} \begin{pmatrix} \mathrm{TE} \\ \mathrm{TM} \end{pmatrix} = 0. \qquad (17)$$

The system above has non-trivial solutions when

$$\Sigma_{xx}\kappa_z - i = 0, \quad \mathrm{TE} = 0 \text{ (TM wave)} \qquad (18)$$

or

$$i\Sigma_{yy} - \kappa_z = 0, \ \text{TM} = 0 \ \text{(TE wave)}. \quad (19)$$

The first of the equations above corresponds to ordinary TM Doppler-shifted mode with dispersion

$$(\omega - ku_0)(\tilde{\omega} - ku_0) = \omega_{2d}^2/\varepsilon, \quad (20)$$

where $\omega_{2d}^2 = 2\pi e^2 n_0 |k_z|/m$ is the fundamental 2d plasma frequency, which we make independent of ε by definition.

In turn, Eq. (19) corresponds to two-dimensional TE galvanomagnetic wave with dispersion

$$\omega_{TE} = \mathbf{k}\mathbf{u}_0 - \frac{i}{\tau_p}\frac{1}{1 + A^2}, \quad (21)$$

where $A = \omega_{2d}/|k_z|c$ is the retardation factor [26–28]. We notice, that $\text{Im}\,\sigma_{xx}(\omega_{TE}) > 0$ whereas $\text{Im}\,\sigma_{yy}(\omega_{TE}) < 0$, which does not contradict the Fal'ko's and Khmel'nitskii's condition (2) derived for isotropic 2DESs.

We observe that Eqs. (1) and (21) have very much in common. Actually, the 3D dispersion (1) was derived for static conductivity, and the account for its dynamic part would lead to the analogue of Eq. (21) with the only change $\omega_{2d} \to \omega_{3d} = \sqrt{4\pi e^2 n_{3d}/m}$, n_{3d} – 3D plasma carrier density.

As a matter of fact, even for $\alpha \neq 0$ the same dispersion (21) holds in the most relevant limit $u_0/c \ll \ll 1, kc \gg \omega, \omega_{2d}$ (please refer to the Supplemenatry material, Section II). To illustrate this statement, we provide a numerical solution to Eq. (16) for a 2DES in GaAs/AlGaAs heterostructure on Fig. 2 with typical parameters enlisted in the figure caption. In this case the eigenmode profile would be TE, TM-mixed.
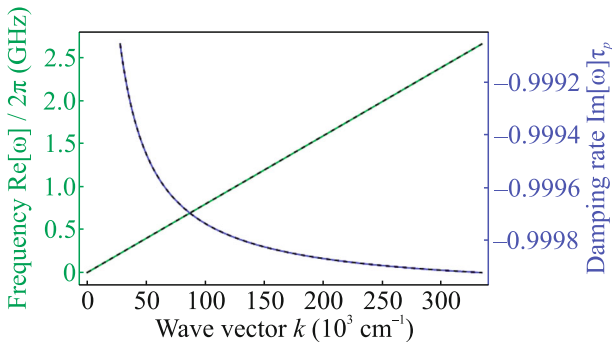

Fig. 2. (Color online) Numerical solution (solid lines) to Eq. (16) and theoretical curves Eq. (21) for an GaAs/AlGaAs heterostructure with parameters $m* = = 0.067 m_e$, m_e is the free electron mass, $\varepsilon = 1$ for simplicity, $n_0 = 10^{12}\,\text{cm}^{-2}$, $u_0 = 10^5\,\text{cm/s}$, $\alpha = \pi/3$, $\tau_p = 1\,\text{ps}$

The main difference between 2D and 3D GMWs is quantitative, which is illustrated in Fig. 3. From this

Figure, blue axis, we observe that GMWs become low-loss in the long wave length limit, and in this limit the 3D GMW loss is approximately $n_{3d}/n_{2d} = 10^6$ times lower than the 2D GMW loss.
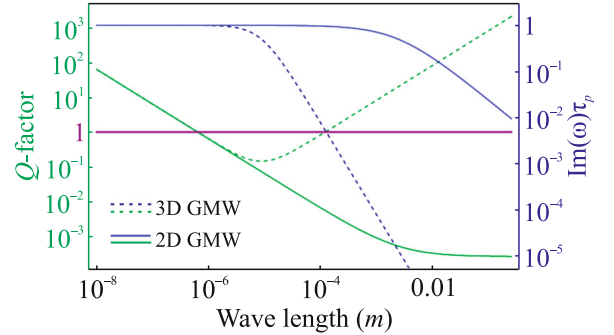

Fig. 3. (Color online) Comparison of 2D and 3D GMWs' Q-factors and damping rates. Green lines correspond to green axis, blue lines – to the blue axis. The purple line denotes $Q = 1$ as an eye-guide for the green axis. Parameters of calculation are the same as in Fig. 2 except for the drift velocity, which is taken to be 10^7 cm/s (approximately the GaAs saturation velocity) and $\alpha = 0$

At the same time, even in the long wave length limit (see Fig. 3) the 2D GMW's Q-factor is extremely small due to coinciding dependencies of real and imaginary parts of frequency on the wave vector: $\text{Re}\,\omega \propto k$ and $\text{Im}\,\omega \propto A^{-2} \propto k$, the latter relation being the consequence of 2D fundamental frequency square-root dispersion. This small value could be increased by larger dc drift (rising $\text{Re}\,\omega$) or higher carrier densities (decreasing $\text{Im}\,\omega$), though even at extremal values the Q-factor is around 10^{-3}. A more intricate way to lower the 2D GMW's loss could be the introduction of magnetic environment [29–31] which is unachievable for 3D GMWs. Our estimates show that the magnetic environment lowers the retardation factor by square root of magnetic permittivity, which could add an order of magnitude to the Q factor at most. Further exploration of the influence of magnetic surrounding on the 2D GMWs would be given elsewhere.

1.3. Interaction of a drift-biased 2DES with EM waves. The found TE GMW posesses the common feature of TE waves: it decreases the reflection of an incident wave [2, 11]. As an example we consider an evanescent wave $\mathbf{E}_{ev} = E_0 \mathbf{e}_y e^{-i\omega t + ik_x x + k_z z}$ incident on a system of Fig. 1. The evanescent wave can be obtained, e.g., in Otto configuration (like it was done in [11]). As a result, reflected and transmitted waves appear:

$$\mathbf{E}_{r,t} = \{r, t\} E_0 \mathbf{e}_y e^{-i\omega t + ik_x x \mp k_z z}. \quad (22)$$

The boundary conditions on the 2DES read:

$$1 + r = t; \qquad (23)$$

$$-1 + r + t = \frac{2i\omega}{k_z c} \frac{2\pi\sigma_{yy}}{c} t, \qquad (24)$$

from which we obtain the reflection coefficient:

$$r = \frac{A^2}{A^2 + \frac{\tilde{\omega} - \mathbf{k}\mathbf{u}_0}{\omega - \mathbf{k}\mathbf{u}_0}}. \qquad (25)$$

We observe that at $\omega = \mathbf{k}\mathbf{u}_0$ the reflection coefficient vanishes (and the transmission coefficient is equal to unity). This means that when the "resonance condition" $\omega = \mathbf{k}\mathbf{u}_0$ is fulfilled, the incident wave does not feel the 2d system and freely passes through it, which is in contrast to ordinary plasmons. In real experiments, however, the reflection coeffient would not be exactly zero at the "TE resonance" as there is always a contrast of dielectric permittivities $\varepsilon_1 \neq \varepsilon_2$.

We also solved a problem when the in-plane wave vector of an incident TE wave is not parallel to the drift: $\mathbf{k} = \mathbf{e}_x k \cos\alpha + \mathbf{e}_y k \sin\alpha$. In this case, the incident wave experiences birefringence and in addition to TE-polarized wave there appears a TM-polarized wave (10) in reflection and transmission signals. The corresponding transmission and reflection coefficients ($r_{TE,TM}$ and $t_{TE,TM}$, respectively) are routinely found from Maxwell's equations.

In Figure 4 we plot the normalized reflection coefficient $|r_{TE}^{ED}|$ of a TE wave (i.e., $\mathbf{E}_{ev} \propto \mathbf{e}_x(-\sin\alpha) + \mathbf{e}_y \cos\alpha$) incident on a 2DES. $|r_{TE}^{ED}|$ is normalized by $|r_{TE}^{QS}|$, where the upper index stands for the conductivity model taken for calculation. From Figure 4 we observe the "TE resonance" line $\omega = \mathbf{k}\mathbf{u}_0$, which corresponds to the condition $r_{TE}^{ED} = 0$, just as in the case of normal incidence $\alpha = 0$, Eq. (25). Obviously, the quasistatic model cannot reproduce this result. The rapid increase of $|r_{TE}^{ED}|/|r_{TE}^{QS}|$ in the lower part of the graph is associated with unphysical dependence $r_{TE}^{QS} \propto \omega$ for low frequencies. Note that the reflection coefficients differ drastically in magnitude.

Interestingly, even in the quasistatic limit, the motherland of $\hat{\sigma}^{QS}$, the quasistatic conductivity tensor may lead to erroneous results. Thus, we found a striking difference between r_{TM}^{QS} and r_{TM}^{ED} in the limit $kc \gg \omega$:

$$r_{TM}^{QS} \equiv 0; \qquad (26)$$

$$r_{TM}^{ED} \propto i|\mathbf{k} \times \mathbf{u}_0|/\omega = iku_0 \sin\alpha/\omega. \qquad (27)$$

From these equations we conclude that the electrodynamic approach predicts the birefringence of an incident TE wave, whereas the quasistatic approach overlooks this effect. In addition, we observe that r_{TM}^{ED} rises
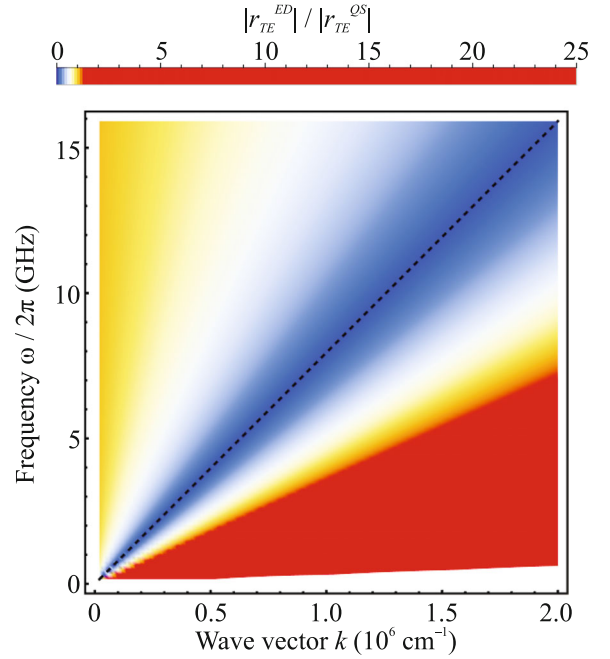

Fig. 4. (Color online) Normalized reflection coefficient $|r_{TE}^{ED}|$ of a TE wave incident on a 2DES obtained with electrodynamic (6) conductivity. The dashed black line corresponds to the real part of TE mode dispersion (21). Parameters of calculation are the same as in Fig. 2. The values are normalized by $|r_{TE}^{QS}|$, the TE reflection coefficient in the same setup calculated with quasistatic conductivity; $|r_{TE}^{QS}|$ is a smooth function in the presented ω, k region

as $1/\omega$ which can be explained in terms of Cerenkov amplification of an incident wave in the low-frequency limit $\omega < ku_0$. A detailed discussion of this effect lies beyond the scope of this Letter and would be presented elsewhere.

2. Final remarks and Conclusion. Our description relies on hydrodynamic Eq. (3). This approximation has a long history [32] and is formally applicable when the electron-electron collision rate ν_{ee} is the dominant rate in the system: $\nu_{ee} \gg \omega/2\pi, 1/\tau_p$. Notably, ν_{ee} can reach the values the order of THz [33], which justifies the apllication of hydrodynamic model in this frequency range and for relatively pure samples ($\tau_p \geq 1\,\text{ps}$). Still, the applicability of the HD approach is even wider, as it corresponds to retaining only the zeroth and first momentum angular harmonics of the distribution function. This approximation becomes asymptotically exact in the long-wavelength limit $kv_F/|\omega + i\nu_{ee}| \ll 1$, where v_F is the Fermi velocity.

Most of our estimates corresponded to drift velocity $u_0 = 10^3\,\text{m/s}$ in GaAs/AlGaAs heterostructures. For typical mobilities order of $\mu = 10\,\text{m}^2/\text{V}\cdot\text{s}$ [34] and char-

acteristic sample size of $L = 100\,\mu$m this value corresponds to $u_0 L/\mu = 10\,$mV of bias voltage.

In conclusion, we studied the interaction of dc charge carrier drift with ac magnetic field in 2DESs (the high-frequency Hall effect) and obtained the previously unknown electrodynamic conductivity tensor $\hat{\sigma}^{ED}$ (6). This tensor is symmetric, in contrast to asymmetric quasistatic conductivity tensor, which implies non-physical chirality. Apart from this fault, the quasistatic model fails to predict birefringence of an incident TE wave on a 2DES even in the quasistatic limit $\omega \ll kc$ as well as Cerenkov amplification; all these effects can be described only by $\hat{\sigma}^{ED}$.

In addition, we showed that the high-freuqency Hall effect leads to the formation of a new electromagnetic mode, the two-dimensional TE galvanomagnetic wave. This wave exists in the vicinity of a 2DES with dc current and has linear dispersion (21). Its damping rate depends on the wave length and can become less than the standard $1/2\tau_p$ 2D fundamental plasmon damping rate in the long wave length limit. Still, the quality factor also fades in this limit at the same rate, which poses an open question for sufficient choice of the 2DES surroundings (e.g., magnetic ones) that could lower the losses. In contrast to 2D TM plasmons, the 2D TE GMW manifests itself in *lowering* the reflection coefficient of an incident EM wave.

Though the quasistatic conductivity can be used for the description of TM plasma waves, we would like to point the inality of this action as the mathematical expressions for $\hat{\sigma}^{QS}$ and $\hat{\sigma}^{ED}$ are of comparable complexity.

We believe that the reported results significantly supplement our understanding of electromagnetic properties of 2DESs with dc current.

Conflict of interest. The authors of this work declare that they have no conflicts of interest.

1. O. V. Konstantinov and V. I. Perel, ZhETF **38**, 161 (1960).

2. B. W. Maxfield, Am. J. Phys. **37**(3), 241 (1969).

3. R. Bowers, C. Legendy, and F. Rose, Phys. Rev. Lett. **7**(9), 339 (1961).

4. R. A. Helliwell and M. G. Morgan, Proceedings of the IRE **47**(2), 200 (1959).

5. A. I. Morozov and P. Shubin, Sov. Phys. JETP **19**, 484 (1964).

6. V. N. Kopylov, JETP Lett. **29**(1), 23 (1979).

7. L. E. Gurevich and B. L. Gelmont, ZhETF **46**, 884 (1964).

8. V. N. Kopylov, JETP Lett. **28**(3), 121 (1978).

9. V. I. Falko and D. E. Khmelnitskii, ZhETF **95**, 847 (1989).

10. S. A. Mikhailov and K. Ziegler, Phys. Rev. Lett. **99**(1), 016803 (2007).

11. S. G. Menabde, D. R. Mason, E. E. Kornev, C. Lee, and N. Park, Sci. Rep. **6**(1), 21523 (2016).

12. I. M. Moiseenko, V. V. Popov, and D. V. Fateev, J. Phys. Condens. Matter **34**(29), 295301 (2022).

13. I. M. Moiseenko, V. V. Popov, and D. V. Fateev, J. Phys. Condens. Matter **35**(25), 255301 (2023).

14. P. S. Alekseev and A. P. Alekseeva, Phys. Rev. Lett. **123**(23), 236801 (2019).

15. D. A. Bandurin, E. Mönah, K. Kapralov, I. Y. Phinney, K. Lindner, S. Liu, J. H. Edgar, I. A. Dmitriev, P. Jarillo-Herrero, D. Svintsov, and S. D. Ganichev, Nat. Phys. **18**(4), 462 (2022).

16. K. Kapralov and D. Svintsov, Phys. Rev. B **106**(11), 115415 (2022).

17. A. B. Mikhailovskii, *Electromagnetic instabilities in an inhomogeneous plasma*, IOP Publishing Bristol, Philadelphia and N.Y. (1992).

18. J. Pozhela, *Plasma and Current Instabilities in Semiconductors: International Series on the Science of the Solid State*, Pergamon Press, Oxford, N.Y., Toronto, Sydney, Paris, Frankfurt (1981), v. 18.

19. M. Dyakonov and M. Shur, IEEE Trans. Electron Devices **43**(3), 380 (1996).

20. V. Yu. Kachorovskii and M. S. Shur, Solid-State Electronics **52**(2), 182 (2008).

21. M. I. Dyakonov, Semiconductors **42**, 984 (2008).

22. O. Sydoruk, R. R. A. Syms, and L. Solymar, Appl. Phys. Lett. **97**(26), 263504 (2010).

23. A. S. Petrov and D. Svintsov, Phys. Rev. B **99**(19), 195437 (2019).

24. A. S. Petrov and D. Svintsov, Phys. Rev. Appl. **17**(5), 054026 (2022).

25. S. A. Mikhailov, Phys. Rev. **58**(3), 1517 (1998).

26. I. Kukushkin, J. Smet, S. A. Mikhailov, D. Kulakovskii, K. von Klitzing, and W. Wegscheider, Phys. Rev. Lett. **102**(8), 081301 (2020).

27. V. Muravev, P. Gusikhin, A. Zarezin, A. Zabolotnykh, V. Volkov, and I. Kukushkin, Phys. Rev. **102**(8), 081301 (2020).

28. I. V. Zagorodnev, A. A. Zabolotnykh, D. A. Rodionov, and V. A. Volkov, Nanomaterials **13**(6), 975 (2023).

29. I. S. Sokolov, D. V. Averyanov, O. E. Parfenov, A. N. Taldenkov, I. A. Karateev, A. M. Tokmachev, and V. G. Storchak, J. Alloys Compd. **884**, 161078 (2021).

30. I. S. Sokolov, D. V. Averyanov, O. E. Parfenov, A. N. Taldenkov, M. G. Rybin, A. M. Tokmachev, and V. G. Storchak, Small **19**, 2301295 (2023).

31. I. S. Sokolov, D. V. Averyanov, O. E. Parfenov, A. N. Taldenkov, A. M. Tokmachev, and V. G. Storchak, Carbon **218**, 118769 (2024).

32. A. D. Boardman, *Electromagnetic surface modes*, John Wiley & Sons Chichester, N. Y., Brisbane, Toronto, Singapore (1982).

33. L. Zheng and S. D. Sarma, Phys. Rev. B **53**, 9964 (1996).

34. V. M. Muravev and I. V. Kukushkin, Phys.-Uspekhi **63**(10), 975 (2020).